journal of materials processing technology 209 (2009) 2180–2185

journal homepage: www.elsevier.com/locate/jmatprotec

A mechanical model for the quantification of the effect of laser quenching on CTOD in steels

Ban-Quan Yang[a,b,c,*], Guang-Nan Chen[b], Kun Zhang[b], Geng-Xing Luo[b], Jing-Hua Xiao[b]

[a] *Division of Engineering Mechanics, Department of Mechanical Engineering, Armored Force Engineering Institute, No. 21, Du Jia Kan, Chang Xin Dian, Beijing 100072, PR China*
[b] *Laboratory of Surface Modification, Institute of Mechanics, Chinese Academy of Sciences, No. 15 Bei si huan xi Road, Beijing 100190, PR China*
[c] *Graduate School of the Chinese Academy of Sciences, Beijing 100190, PR China*

ARTICLE INFO

Article history:
Received 15 March 2007
Received in revised form
22 April 2008
Accepted 4 May 2008

Keywords:
Laser quenching
Crack tip opening displacement (CTOD)
Residual stress gradient effect
Micro-hardness
Steels

ABSTRACT

The technology of laser quenching is widely used to improve the surface properties of steels in surface engineering. Generally, laser quenching of steels can lead to two important results. One is the generation of residual stress in the surface layer. In general, the residual stress varies from the surface to the interior along the quenched track depth direction, and the residual stress variation is termed as residual stress gradient effect in this work. The other is the change of mechanical properties of the surface layer, such as the increases of the micro-hardness, resulting from the changes of the microstructure of the surface layer. In this work, a mechanical model of a laser-quenched specimen with a crack in the middle of the quenched layer is developed to quantify the effect of residual stress gradient and the average micro-hardness over the crack length on crack tip opening displacement (CTOD). It is assumed that the crack in the middle of the quenched layer is created after laser quenching, and the crack can be a pre-crack or a defect due to some reasons, such as a void, cavity or a micro-crack. Based on the elastic–plastic fracture mechanics theory and using the relationship between the micro-hardness and yield strength, a concise analytical solution, which can be used to quantify the effect of residual stress gradient and the average micro-hardness over the crack length resulting from laser quenching on CTOD, is obtained. The concise analytical solution obtained in this work, cannot only be used as a means to predict the crack driving force in terms of the CTOD, but also serve as a baseline for further experimental investigation of the effect after laser-quenching treatment on fracture toughness in terms of the critical CTOD of a specimen, accounting for the laser-quenching effect. A numerical example presented in this work shows that the CTOD of the quenched can be significantly decreased in comparison with that of the unquenched.

* *Corresponding author.*
E-mail address: yangbq1022@tom.com (B.-Q. Yang).
0924-0136/$ – see front matter
doi:10.1016/j.jmatprotec.2008.05.018

1. Introduction

In surface engineering, laser quenching is widely used to improve the surface properties of steels (Ion, 2002), such as the fatigue properties (Heitkemper et al., 2003; Cruz et al., 1998), wear properties (Pantelis et al., 2002; Shao et al., 2003) and erosion properties (Chong et al., 2003; Lo et al., 2003). Generally, laser quenching of steels can lead to two important results. One is the generation of residual stress in the surface layer. The residual compressive stress on the quenched steel surface and in the surface layer down to a certain depth could range between 200 and 500 MPa (Grum and Žerovnik, 1993a,b). Generally, the residual stress varies from the surface to the interior along the quenched track depth direction, and when it reaches a certain depth, it transforms from compressive to tensile (Grum and Žerovnik, 1993a,b). In this work, the residual stress variation is termed as residual stress gradient effect. The other is the change of microstructure. The grain size of laser-hardened zone is much smaller than that of the traditional quenched high-speed steels at different quenching temperatures (Shi et al., 1995). This finer microstructure could be obtained by using optimum processing parameters (Liu and Liu, 1999). The desirable microstructure, which contains fewer weak sites, can exhibit a favorable combination of hardness and toughness (Lo et al., 2003). The changes of microstructure can lead to changes of mechanical properties, such as the increases of the yield strength and micro-hardness. Authors (Kolednik and Suresh, 1999; Kolednik, 2000) stated that variations in yield strength could appear in welded structures, soldered joints, nitrided or case-hardened components and so on, and presented an yield strength gradient term of the crack driving force in terms of J-integral. Hardness, the important property, can be increased greatly, and it can be measured directly or predicted by a mathematical model (Guan et al., 1997). Apart from the wear and erosion experiments, it should be emphasized that most of the experiments in the studies mentioned above were restricted to the fatigue property research under dynamic loads. Recently, a mechanical model was developed to quantify the effect of laser quenching on crack driving force in terms of J-integral, and it could be obtained that the dominant factor influencing the crack driving force was the residual stress (Yang et al., 2006, 2007). However, the residual stress is approximated as a mean value over the crack length, and the residual stress gradient effect was not considered in (Yang et al., 2006, 2007). Also, the results presented in (Yang et al., 2006, 2007) are suitable for the case that the crack tip is in the middle of the hardened layer, and they are not suitable for the cases that the crack tip is in the transitional layer, heat-affected layer or base material. In this work, a two-dimensional mechanical model, based on elastic–plastic fracture mechanics theory, is developed that allows us to derive a concise analytical solution to quantify the effect of residual stress gradient and the average micro-hardness over the crack length resulting from laser quenching on CTOD for a given crack length. The crack tip opening displacement (CTOD) fracture criterion is one of the oldest fracture criteria applied to fracture of metallic materials with cracks (Newman et al., 2003), and the standard CTOD test methods and procedure can be found in (BS5762, 1979). The theoretical analysis presented in work is essential to predict the crack driving force in terms of CTOD of a specimen after laser-quenching treatment, and it is also essential to further experimental investigation of the effect after laser-quenching treatment on fracture toughness in terms of the critical CTOD of a specimen.

2. The mechanical model

The treatment way of laser quenching of steels can be in the form of laser scanning. Here, the laser-scanning track is assumed to be periodic for relatively large size flat workpieces, and the interaction between the tracks is ignored for simplicity. We can thus choose a representative track as our study objective of interest. We can also choose a representative track for the flat workpieces, as their surface dimension in any direction is smaller than or equal to that of the laser track. Laser quenching makes steel a more functional material as the laser-quenched layer is composed of a hardened zone, a transition zone and a heat-affected zone, each zone having different properties (Obergfell et al., 2003). The hardened zone is composed of a completely martensitic structure; the transition zone consisted of a partly austenitised and eventually hardened structure and material fractions that did not transform to austenite during the laser irradiation; and the heat-affected zone depended on the state of the unaffected base material (Obergfell et al., 2003). The shape of the cross-section of the laser-quenched zone is simplified, and the cross-section of the laser-quenched zone is schematically illustrated in Fig. 1, in which h denotes the total depth of the laser-quenched layer. Generally, the total depth of the laser-quenched layer can vary from the order of micron to centimeter. Many factors may affect the total depth of the laser-quenched layer, such as the laser power density, the diameter of the laser spot and the laser scanning speed. In this work, the mechanical property, Young's modulus E, is assumed to be invariant in the four zones since the general heat treatments have little influence on Young's modulus of metals besides the laser quenching (Meyers and Chawla, 1984).

As shown in Fig. 2, it is assumed that there exists a crack in the middle of the quenched layer, which will propagate along the quenched depth direction. The crack can be a pre-crack

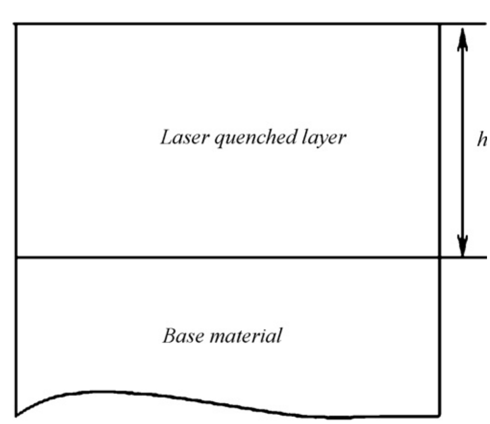

Fig. 1 – A schematic illustration of the cross-section of a representative track.

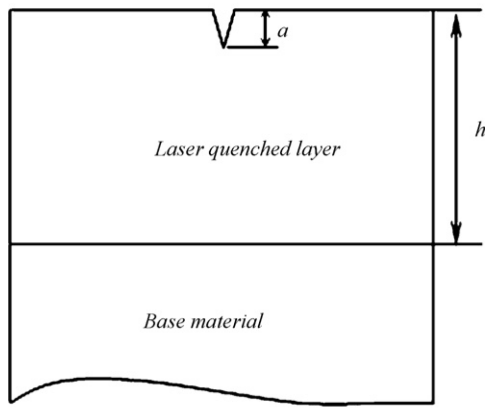

Fig. 2 – A schematic illustration of a crack in the middle of the quenched layer.

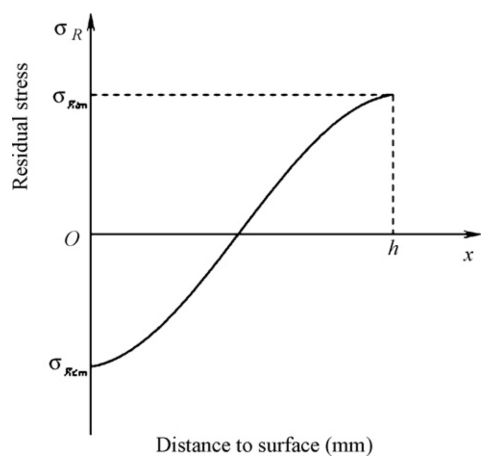

Fig. 3 – Residual stress as a function of the quenched track depth.

or a defect due to some reasons, such as a void, cavity or a micro-crack. This is a reasonable assumption since the surface and subsurface crack initiations occur independently of the applied load level, as stated in (Cruz et al., 1998). Since the residual stress is the dominant factor that influences the crack driving force (Yang et al., 2006, 2007), the micro-hardness is approximated as an average value over the crack length for simplicity in this work.

In this study, let x be the abscissa denoting the quenched track depth direction, and the residual stress as a function of the quenched track depth x can be written as

$$\sigma_R = \sigma_R(x) \tag{1}$$

Residual stress in the middle of the quenched track as a function of the quenched track depth x is illustrated in Fig. 3, in which σ_{Rcm} denotes maximum residual compressive stress and σ_{Rtm} denotes maximum residual tensile stress. In this work, the residual compressive stress is a negative value, and the residual tensile stress is a positive value. One specific law of a residual stress variation is given in Section 4 of the paper.

As illustrated in Fig. 4, a pre-cracked body with a constant thickness consisting of non-linear elastic material that

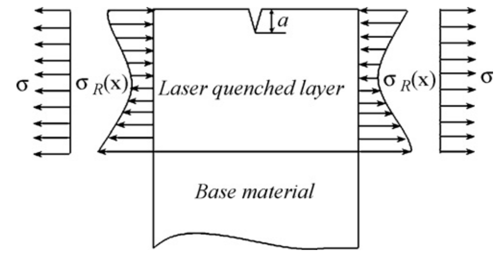

Fig. 4 – The mechanical model.

has the same stress–strain response during the loading as an elastic-perfectly plastic material with a yield strength, σ_s, is considered. The crack length, a, is assumed to be less than h, i.e. $a < h$. The external stress σ and the residual stress are applied at infinity of the body.

3. Analytical solution

The Dugdale model (Dugdale, 1960) describing the crack contour can be shown in Fig. 5. Based on the elastic–plastic fracture mechanics, the plastic zone size ρ can be given as (Dugdale, 1960):

$$\rho = a\left(\sec\frac{\pi\sigma}{2\sigma_s} - 1\right) \tag{2}$$

And the CTOD of a crack in an infinite body is (Dugdale, 1960)

$$\mathrm{CTOD} = \frac{8\sigma_s a}{\pi E_1}\ \ln\left(\sec\frac{\pi\sigma}{2\sigma_s}\right) \tag{3}$$

where $E_1 = E$ identifies with Young's modulus in plane stress. In the case of plane strain problem, E_1 is replaced by $E/(1-\nu^2)$, with ν being the Poisson ratio.

For the small-scale-yielding condition, i.e. $\sigma/\sigma_s \leq 0.6$, under the external stress, σ, the CTOD of a crack in an infinite body

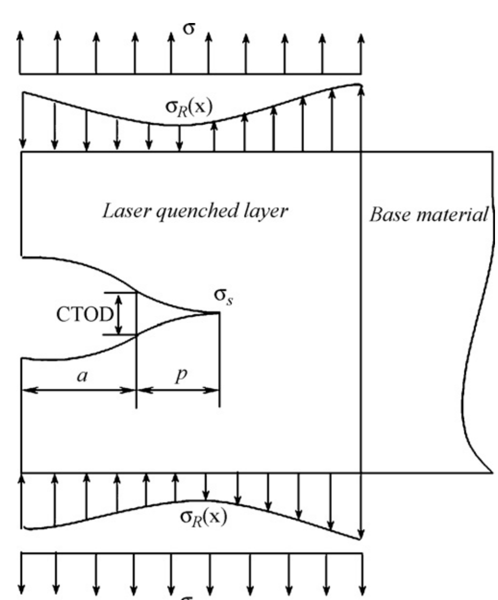

Fig. 5 – The Dugdale model describing the crack contour.

can be derived from Eq. (3) (Dugdale, 1960):

$$\mathrm{CTOD} = \frac{\pi a}{E_1 \sigma_s} \sigma^2 \tag{4}$$

In this work, due to the edge crack in a semi-infinite body, the crack tip opening displacement can be multiplied by a modifying dimensionless coefficient M, which depends on the geometry of the pre-cracked body. Thus, Eqs. (3) and (4), becomes respectively:

$$\mathrm{CTOD} = M \frac{8\sigma_s a}{\pi E_1} \ln\left(\sec \frac{\pi\sigma}{2\sigma_s}\right) \tag{5}$$

$$\mathrm{CTOD} = M \frac{\pi a}{E_1 \sigma_s} \sigma^2 \tag{6}$$

However, Eqs. (5) and (6) do not include the term of the residual stress that influences the CTOD. By using the superposition principle, the external stress σ in Eqs. (5) and (6) can be replaced by$\sigma + \sigma_R$, and the small-scale-yielding condition changed as. $(\sigma + \sigma_R)/\sigma_s \le 0.6$. Thus, the Eqs. (5) and (6) can be written respectively as

$$\mathrm{CTOD} = M \frac{8\sigma_s a}{\pi E_1} \ln\left[\sec \frac{\pi(\sigma + \sigma_R)}{2\sigma_s}\right] \tag{7}$$

$$\mathrm{CTOD} = M \frac{\pi a \sigma^2}{E_1 \sigma_s} \left(1 + \frac{\sigma_R}{\sigma}\right)^2 \tag{8}$$

Here, it should be emphasized that, for materials treated by laser quenching, it is very difficult to measure the yield strength for a particular point along the quenched track depth direction directly. Thus, it may be hard to obtain the law of the variable yield strength in a microzone from a practical viewpoint. However, the measurement of the micro-hardness is easy and quick. In addition, the micro-hardness could be approximated as three times of the yield strength for metal materials under the condition that the working hardening could be neglected, as stated in (Tabor, 1951; Ashby and Jones, 1980). Recently, using dimensional analysis and finite element calculations, authors (Cheng and Cheng, 1998, 1999, 2004) stated that the yield strength could be estimated directly from the hardness measurement in practice, and the relationship between the hardness and yield strength has been discussed in detail in Cheng and Cheng (1998, 1999). For a given material, the specific relationship between the micro-hardness and yield strength can be written as (Tabor, 1951; Ashby and Jones, 1980; Cheng and Cheng, 1998, 1999, 2004):

$$\sigma_s = kH \tag{9}$$

where k is a dimensionless coefficient. For a given material, the coefficient k depends on the properties of the material and can be determined by experiment (Tabor, 1951) or finite element calculations (Cheng and Cheng, 1998, 1999, 2004). In the case of the elastic-perfectly plastic metals, for most metals for which $0 < \sigma_s/E < 0.01$ (E is the Young's modulus), k is between 1/2.6 and 1/2.5, as stated in (Cheng and Cheng, 1999). For a variety of materials, k can range from 1/2.8 to 1/1.7, but for most metals for which $0 < \sigma_s/E < 0.01$, k approximates 1/2.8, as stated in (Cheng and Cheng, 1998). But authors (Tabor, 1951; Ashby and Jones, 1980) stated that the coefficient k could be approximated as 1/3 under the condition that the working hardening could be neglected.

Here, let H_{av} denote the average hardness over the crack length, and H in Eqs. (9) can be replaced by H_{av}. Substituting Eq. (9) into Eqs. (7) and (8) yields, respectively:

$$\mathrm{CTOD} = M \frac{8kH_{av} a}{\pi E_1} \ln\left[\sec \frac{\pi(\sigma + \sigma_R)}{2kH_{av}}\right] \tag{10}$$

$$\mathrm{CTOD} = M \frac{\pi a \sigma^2}{E_1 k H_{av}} \left(1 + \frac{\sigma_R}{\sigma}\right)^2 \tag{11}$$

Thus, the desirable analytical solutions, which can be used to quantify the effect of residual stress and the average hardness over the crack length resulting from laser-quenching treatment on CTOD, is obtained. Here, it should be emphasized that Eq. (11) is only suitable for the small-scale-yielding condition.

4. A numerical example

A numerical example shall investigate the residual stress gradient influence the crack driving force. In some cases, at a depth between 300 and 600 μm, the residual compressive stress transforms itself into tensile residual stress, and the tensile residual stress can reach 500 MPa (Grum and Žerovnik, 1993a,b). Here, it is assumed that the variation law of the residual stress as a function of depth approximately satisfies a polynomial expression:

$$\sigma_R(x) = A_0 + A_1 x + A_2 x^2 \tag{12}$$

where A_0, A_1 and A_2 are coefficients to be determined. For a particular case, it is assumed that when $x = 0$, the maximum residual compressive stress $\sigma_{Rcm} = -500$ MPa, when $x = 4 \times 10^{-4}$ m, $\sigma_R = 0$ and when $x = 6 \times 10^{-4}$ m, the maximum residual tensile stress $\sigma_{Rtm} = -500$ MPa. Using curve fitting, these coefficients can be determined and they are

$$A_0 = -5 \times 10^8, \quad A_1 = 4.1667 \times 10^{11}, \quad A_2 = 2.0833 \times 10^{15}$$

Thus, the residual stress as a function of the depth has been determined. For this particular case in this work, the plot of residual stress as a function of the depth is shown in Fig. 6, in which where $0 \le x < 4 \times 10^{-4}$ m, the residual compressive stress exists, and where $4 \times 10^{-4}\ \mathrm{m} < x \le 6 \times 10^{-4}$ m, the residual tensile stress exists.

One of the hardness distribution characteristics in the middle of the quenched track along the quenched track depth direction is taken from reference Grum and Žerovnik (1993a,b), in which the maximum micro-hardness H_{max} can approximately equal to 7000 MPa, and the micro-hardness of the base material H_{min} can approximately equal to 2000 MPa.

Under the same external loading conditions, the quenched and the unquenched steel (without laser-quenching treatment) share a same crack length a. It is assumed that the crack length a equals to 0.1 mm, the external stress σ equals to 500 MPa, and the average micro-hardness H_{av} over the crack length equals to 4500 MPa. Given these conditions, the ratio of the CTOD of the quenched layer to that of the unquenched

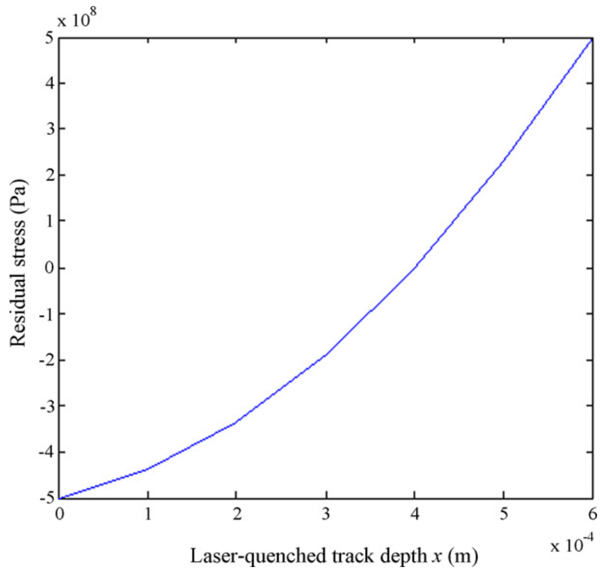

Fig. 6 – A variation law of the residual stress as a function of the depth.

layer can be calculated from Eq. (10), and the result shows that the CTOD of the quenched specimen is nearly 1/18 of the unquenched. This means that the residual compressive stress and higher micro-hardness resulting from laser quenching can significantly decrease the CTOD.

5. Results and discussions

In Eqs. (10) and (11), it is defined that $\sigma + \sigma_R > 0$, and it can be seen that the CTOD decreases with the increase of H_{av} or (and) residual compressive stress σ_R. So from these results, it can be seen that the higher residual compressive stress and higher micro-hardness resulting from laser-quenching treatment can decrease much more CTOD. This is a reasonable trend. If $\sigma + \sigma_R < 0$, i.e. the absolute value of the residual compressive stress is larger than the external tensile stress, it would be the crack closure/contact problem, and the problem is beyond the scope of this work.

On the contrary, if the residual stress is tensile, CTOD will increase significantly with the increase of residual tensile stress. In this case, the tensile stress will adversely enlarge the CTOD, and it can be detrimental to the workpieces. Thus, it can be concluded that the mechanical model presented in this paper is reasonable, and the results presented in this work can be used to quantify the residual stress gradient effect and the average micro-hardness over the crack length after laser quenching on crack driving force in terms of CTOD.

In addition, if the distribution law of the residual stress and average micro-hardness over the crack length can be determined, the concise analytical solution can be used to study the laser-quenching effect on fracture toughness of a quenched specimen, accounting for the laser-quenching effect. The residual stress in the middle of the quenched track as a function of quenched track depth is assumed to satisfy a polynomial expression law. One can also take other formulas to approximately express the law of the residual stress variation along the quenched track depth direction for a specific or practical case.

For elastic–plastic fracture mechanics, there is a correlation between the CTOD and the parameter *J*-integral (Anderson, 1995), i.e. CTOD = J/σ_S. However, this equation is valid for material exhibiting homogeneous yield strength, and it is not valid for the case that the yield strength varies with the layer depth, i.e., there is a yield strength gradient.

The model presented in this work is suitable for all kinds of quenched steels, and the results are suitable for the case that the crack tip is in the middle of the hardened layer, transitional layer or heat-affected layer. Also, the results presented in this work are not only limited to the case of laser-quenching treatment, they can also be extended to other forms of high-energy surface treatments, such as electron beam surface treatment, ion beam surface treatment, and so on.

6. Conclusions

A mechanical model is developed to quantify the residual stress gradient effect and the average micro-hardness over the crack length after laser-quenching treatment on CTOD from the standpoint of fracture mechanics. From the concise analytical solution, it can be seen that the CTOD decreases with the increase(s) of residual compressive stress or (and) the average micro-hardness over the crack length. From the numerical analysis, it can be obtained that the CTOD of the quenched can be greatly decreased in comparison with that of the unquenched.

The concise analytical solution in this work, cannot only be used as a means to predict the crack driving force in terms of the CTOD, but also serve as a baseline for further experimental investigation of the effect after laser-quenching treatment on fracture toughness in terms of the critical CTOD of a specimen, accounting for the laser-quenching effect.

The results presented in this work can also be applied to other forms of high-energy surface treatments.

Acknowledgement

The financial support provided by the National Natural Science Foundation of China (Grant No. 50531060) is greatly acknowledged.

REFERENCES

Anderson, T.L., 1995. Fracture Mechanics. CRC Press.
Ashby, M.F., Jones, D.R.H., 1980. Engineering Materials. Oxford Pergamon Press, London, p. 105.
BS5762, 1979. Methods for crack opening displacement (COD) testing. British Standards Institution, London.
Cheng, Y.T., Cheng, C.M., 1998. Scaling approach to conical indentation in elastic–plastic solids with work hardening. J. Appl. Phys. 84, 1284–1291.
Cheng, Y.T., Cheng, C.M., 1999. Scaling relationships in conical indentation of elastic-perfectly plastic solids. Int. J. Solids Struct. 36, 1231–1243.
Cheng, Y.T., Cheng, C.M., 2004. Scaling, dimensional analysis, and indentation measurements. Mater. Sci. Eng. R 44, 91–149.

Chong, P.H., Liu, Z., Skeldon, P., Thompson, G.E., 2003. Large area laser surface treatment of aluminium alloys for pitting corrosion protection. Appl. Surf. Sci. 208–209, 399–404.
Cruz, P.D., Odén, M., Ericsson, T., 1998. Effect of laser hardening on the fatigue strength and fracture of a B–Mn steel. Int. J. Fatigue 20, 389–398.
Dugdale, D.S., 1960. Yielding of steel sheets containing slits. J. Mech. Phys. Solids 8, 100–104.
Grum, J., Žerovnik, P., 1993a. Laser hardening steels-Part 1. Heat Treat. 25, 16–20.
Grum, J., Žerovnik, P., 1993b. Laser hardening steels-Part 2. Heat Treat. 25, 32–36.
Guan, Y.H., Chen, T.L., Wang, H.G., Zhang, J.T., 1997. The prediction of the mechanical properties of metal during laser quenching. J. Mater. Process. Technol. 63, 614–617.
Heitkemper, M., Bohne, C., Pyzalla, A., Fischer, A., 2003. Fatigue and fracture behavior of a laser surface heat treated martensitic high-nitrogen tool steel. Int. J. Fatigue 25, 101–106.
Ion, J.C., 2002. Laser transformation hardening. Surf. Eng. 18, 14–31.
Kolednik, O., 2000. Yield stress gradient effect in inhomogeneous materials. Int. J. Solids Struct. 37, 781–808.
Kolednik, O., Suresh, S., 1999. Influence of the yield strength gradient on the fracture resistance in FGMs. Mater. Sci. Forum 308–311, 963–970.
Liu, Q.B., Liu, H., 1999. Experimental study of the laser quenching of 40CrNiMoA steel. J. Mater. Process. Technol. 88, 77–82.
Lo, K.H., Cheng, F.T., Man, H.C., 2003. Laser transformation hardening of AISI 440C martensitic stainless steel for higher cavitation erosion resistance. Surf. Coat. Technol. 173, 96–104.
Meyers, M.A., Chawla, K.K., 1984. Mechanical Metallurgy. Prentice Hall, New Jersey.
Newman, J.C., James, M.A., Zerbst, U., 2003. A review of the CTOA/CTOD fracture criterion. Eng. Fract. Mech. 33, 371–385.
Obergfell, K., Schulze, V., Vöhringer, O., 2003. Classification of microstructural changes in laser hardened steel surfaces. Mater. Sci. Eng. A 355, 348–356.
Pantelis, D.I., Bouyiouri, E., Kouloumbi, N., Vassiliou, P., Koutsomichalis, A., 2002. Wear and corrosion resistance of laser surface hardened structural steel. Surf. Coat. Technol. 298, 125–134.
Shao, T.M., Hua, M., Yuen, T.H., 2003. Impact wear behavior of laser hardened hypoeutectoid 2Cr13 martensite stainless steel. Wear 255, 444–455.
Shi, G.Q., Ding, P.D., Liu, J.L., Yin, H.J., Wang, J., 1995. Microstructure and properties of laser surface hardened M2 high speed steel. Acta. Metall. Mater. 43, 217–223.
Tabor, D., 1951. The Hardness of Metals. Oxford University Press, London.
Yang, B.Q., Zhang, K., Chen, G.N., Luo, G.X., Xiao, J.H., 2006. A quantitative analysis of the effect of laser transformation hardening on crack driving force in steels. Surf. Coat. Technol. 201, 2208–2216.
Yang, B.Q., Zhang, K., Chen, G.N., Luo, G.X., Xiao, J.H., 2007. Effect of a laser pre-quenched steel substrate surface on the crack driving force in a coating-steel substrate system. Acta Mater. 55, 4349–4358.